Progress In Electromagnetics Research B, Vol. 4, 197–210, 2008

METHOD OF MOMENT ANALYSIS OF FINITE PHASED ARRAY OF APERTURE COUPLED CIRCULAR MICROSTRIP PATCH ANTENNAS

H. R. Hassani

Electrical & Electronic Engineering Department
Shahed University
Tehran, Iran

M. Jahanbakht

Islamic Azad University
Shahryar-Shahr-e-Qods-Branch, Tehran, Iran

Abstract—A full wave spectral domain method of moment along with reciprocity theorem analysis of finite phased array of aperture coupled circular microstrip patch antennas is presented. Both the electric surface currents on the patches and the equivalent magnetic current on the apertures are considered. Results of reflection coefficient magnitude, active input impedance, active element gain, efficiency and pattern are provided for different array size and element separations. By optimizing the parameters of the array, a better scan performance can be achieved. Furthermore, a comparison is made between array of rectangular and circular patches, with equal patch surface area, and it is shown that the array of circular patches provide a better scan performance than the array of rectangular patches.

1. INTRODUCTION

Due to their many attractive features, printed circuit phased array antennas have received a great deal of attention in the past few years. One of the techniques of feeding such printed circuit antennas is through apertures between the feed line and the patch antennas. This feeding configuration provides many advantages compared to the conventional feeding techniques such as isolating spurious feed radiation by use of a ground plane and allows active devices to be integrated on the feed structure.

Review of the literature shows that there has been a number of published papers on the subject of application of the phased array antennas [1–4], general analysis of phased array [5–8] and analysis of printed phased arrays such as probe fed dipole and rectangular patch antenna in an infinite and finite array format [9–13]. Aperture coupled fed infinite phased array of rectangular patches [14] and finite phased array of stacked circular patches [15] has also been analyzed. In [15] in order to evaluate the characteristics of aperture coupled microstrip antennas in a finite array and derive the moment-method solutions for the unknown current distributions on the patches and slots, the reciprocity theorem and the spectral domain Green's functions for a dielectric slab are used. But this work is pertained to a stacked microstrip patch and neither Green's functions nor results are suitable for a single layer structure. Furthermore, no comparison is made between rectangular and circular patches in a finite array environment.

To the knowledge of the authors no full wave analysis of the aperture coupled finite phased array of rectangular or circular patch antennas is in evidence. It is well known that the infinite array approximation, models the central element of a large but finite array quite well but it is difficult to predict the behavior of the antenna elements positioned near the edges.

In this paper, we present a method of moment analysis of the aperture coupled finite phased array of circular and rectangular microstrip patch antennas in the spectral domain. This uses the exact Green's functions for the structure and takes into account the surface wave effects on both the feed and the patch dielectric substrates. Appropriate basis functions for the current distribution on the patch are considered. The method uses the reciprocity theorem to analyze the coupling of the microstrip feed line to the narrow rectangular slot in the ground plane. Once the current distribution on the circular patch is found, the active Input impedance, active reflection coefficient magnitude, efficiency and active element gain and active element pattern can be obtained. Upon comparison between arrays of rectangular patches to arrays of circular patches it will be shown that for equal surface area of the patches and optimized parameters, the circular patch provides a better scanning performance.

2. THEORY

The geometry of a finite phased array of aperture coupled circular microstrip patch antenna is shown in Fig. 1. The patches are spaced uniformly (and not equally) in the x and y directions. The spectral domain analysis of the finite array is basically similar to that of the

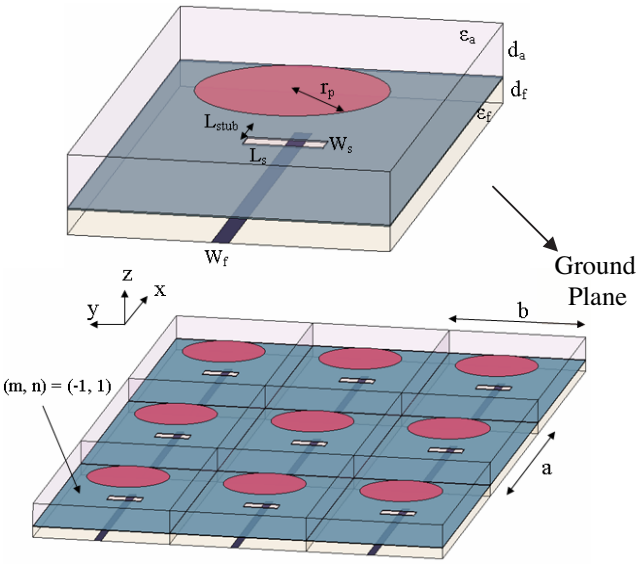

Figure 1. Geometry of a finite phased array of aperture coupled circular microstrip patch antennas.

infinite array formulated in [14], where details of the formulation can be found. For the purpose of completeness the basic analysis procedure for the finite array is outlined below.

The analysis can be divided into two separate parts. The first part is above the ground plane between the slots and the patches and the second part is under ground plane between the feed lines and the slots.

For the first part, the electric field integral equation, EFIE, (based on boundary condition on the perfectly conducting patches, $\overline{E}^{\tan}_{scat}(\overline{J}_s) = -\overline{E}^{\tan}_{inc}(\overline{M}_s)$) for the surface current on the patches is written in terms of the appropriate Green's functions. This is then solved by the Galerkin method of moment in the spectral domain. In the method of moment, the unknown current on the patches in x and y directions are expanded by a series of basis functions. By substituting these basis functions in the EFIE and taking the inner product of the resultant equation with testing functions (similar to basis functions) the final equation would of the form,

$$\sum_{g=1}^{N} Z_{hg} I_g = V_h \qquad (h = 1, 2, \ldots, N) \tag{1}$$

One may express this equation in a matrix operator form as,

$$\begin{bmatrix} Z_{11\,xx} & \dots Z_{1N\,xx} & Z_{11\,xy} & \dots Z_{1N\,xy} \\ \vdots & \vdots & \vdots & \vdots \\ Z_{N1\,xx} & \dots Z_{NN\,xx} & Z_{N1\,xy} & \dots Z_{NN\,xy} \\ Z_{11\,yx} & \dots Z_{1N\,yx} & Z_{11\,yy} & \dots Z_{1N\,yy} \\ \vdots & \vdots & \vdots & \vdots \\ Z_{N1\,yx} & \dots Z_{NN\,yx} & Z_{N1\,yy} & \dots Z_{NN\,yy} \end{bmatrix} \cdot \begin{bmatrix} I_{1x} \\ \vdots \\ I_{Nx} \\ I_{1y} \\ \vdots \\ I_{Ny} \end{bmatrix} = \begin{bmatrix} V_{1\,xy} \\ \vdots \\ V_{N\,xy} \\ V_{1\,yy} \\ \vdots \\ V_{N\,yy} \end{bmatrix} \cdot [I^p] \tag{2}$$

in which

$$I_i^p = e^{jk_0(kau+lbv)}, \quad u = \sin\theta \cdot \cos\phi \quad \text{and} \quad v = \sin\theta \cdot \sin\phi$$

and

$$\begin{aligned} Z_{mn\,xx} &= \frac{1}{4\pi^2} \iint_{-\infty}^{\infty} \tilde{J}_{mx}^* \cdot \tilde{G}_{xx}^{EJ} \cdot \tilde{J}_{nx} \cdot e^{jk_y S_y} \cdot \beta d\alpha d\beta \\ Z_{mn\,xy} &= \frac{1}{4\pi^2} \iint_{-\infty}^{\infty} \tilde{J}_{mx}^* \cdot \tilde{G}_{xy}^{EJ} \cdot \tilde{J}_{ny} \cdot e^{jk_y S_y} \cdot \beta d\alpha d\beta \\ Z_{mn\,xx} &= \frac{1}{4\pi^2} \iint_{-\infty}^{\infty} \tilde{J}_{my}^* \cdot \tilde{G}_{yx}^{EJ} \cdot \tilde{J}_{nx} \cdot e^{jk_y S_y} \cdot \beta d\alpha d\beta \\ Z_{mn\,yy} &= \frac{1}{4\pi^2} \iint_{-\infty}^{\infty} \tilde{J}_{my}^* \cdot \tilde{G}_{yy}^{EJ} \cdot \tilde{J}_{ny} \cdot e^{jk_y S_y} \cdot \beta d\alpha d\beta \\ V_{m\,xy} &= -\frac{1}{4\pi^2} \iint_{-\infty}^{\infty} \tilde{J}_{mx}^* \cdot \tilde{G}_{xy}^{EM} \cdot \tilde{M}_{sy} \cdot \beta d\alpha d\beta \\ V_{m\,yy} &= -\frac{1}{4\pi^2} \iint_{-\infty}^{\infty} \tilde{J}_{my}^* \cdot \tilde{G}_{yy}^{EM} \cdot \tilde{M}_{sy} \cdot \beta d\alpha d\beta \end{aligned} \tag{3}$$

where $\tilde{J}_g$ is the Fourier Transform of the gth basis or testing functions. I_g is the complex unknown vector current coefficient, $\tilde{G}$ is the dyadic Green's function, $\tilde{M}_{sy}$ is the equivalent magnetic current on the slots and ($\sim$) represent Fourier Transform and (*) denotes complex

conjugate. The elements of the Greens functions required are given in the appendix.

In the above analysis for the phased array antenna, each of the array elements is assumed to be fed (scanned) by a source of $e^{jk_0(mau+nbv)}$. The basis functions on each patch suitable for our analysis are similar to those in [14] for rectangular patches and [16] for circular patches and are presented again in the appendix for convenience. The basis functions for the circular patches correspond to the TM_{mn} modes of a circular cavity and are suitable for wave functions with even symmetry. For the narrow slot, the equivalent magnetic current is approximated with a single piece - wise sinusoidal mode,

$$\tilde{M}_{sy} = \tilde{e}_x^a = \frac{\sin(k_x W_s/2)}{k_x W_s/2} \cdot \frac{2k_e[\cos(k_y L_s/2) - \cos(k_e L_s/2)]}{\sin(k_e L_s/2) \cdot \left(k_e^2 - k_y^2\right)} \tag{4}$$

where k_e is the effective wave number.

For the second part of the analysis, coupling between the feed lines and slots can be applied by taking the advantage of the reciprocity theorem [14] in which the couplings between feed lines are neglected. An equivalent circuit for each of the aperture coupled patch antennas can then be considered, as shown in Fig. 2. In this circuit, the series impedance Z is given by,

$$Z = Z_c \cdot \frac{\Delta v^2}{Y^e + Y^a} \tag{5}$$

where Z_c is the characteristic impedance of the microstrip line, the denominator $Y^e + Y^a$ represents the aperture admittance and Δv is a modal voltage for the field over the aperture due to the discontinuity of the slot. The latter is:

$$\Delta v = \int_{S_a} e_x^a(x,y) h_y(x,y) ds = \frac{1}{\sqrt{z_c}} \int_{-\infty}^{\infty} \tilde{F}_u(k_y) \tilde{G}_{yx}^{HJ}(-k_e, k_y) \tilde{F}_p(k_y) dk_y \tag{6}$$

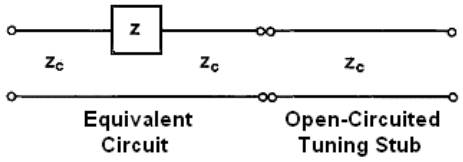

Figure 2. The equivalent circuit of aperture coupled patch antenna as seen by the microstrip feed line.

where s_a is the surface of the aperture and $\tilde{F}_u$ and $\tilde{F}_p$ are the spectral domain expressions for the transverse and piecewise sinusoidal current distributions on the feed line and aperture, respectively [14]. Y_e, is the self admittance of the slot, representing the reaction between slot electric field and the magnetic field radiated by the aperture towards the feed line (f) and patch antenna (a) and is expressed as:

$$\begin{aligned} Y^e &= \int_{s_a} e_x^a(x,y) H_y^M ds \\ &= \frac{1}{4\pi} \iint_{-\infty} \tilde{F}_u^2(k_x)(\tilde{G}_{yy}^{HM(f)}(k_x,k_y) + \tilde{G}_{yy}^{HM(a)}(k_x,k_y))\tilde{F}_p^2(k_y) dk_x dk_y \end{aligned} \tag{7}$$

and Y^a represents the reaction between the slot electric field and the magnetic field scattered due to the current on the patch and can be expressed as,

$$Y^a = \int_{s_a} e_x^a(x,y) H_y ds = [V]^t [Z]^{-1} [V] \tag{8}$$

Upon substitution in Equation (5), the series impedance Z of Fig. 2 is obtained. Aperture coupled patch antenna is usually tuned with an open-circuited stub of Microstrip line. If the stub length is L_{stub}, using transmission line theory, the input impedance referenced to the aperture would be,

$$Z_{in}(\theta,\varphi) = Z - jZ_c \cdot \cot(\beta L_{stub}) \tag{9}$$

where β is the propagation constant of the feed line. More accurate results can be obtained by adding a length extension to L_{stub} to account for fringing fields at the end of the open stub. Then the active reflection coefficient can be obtained from,

$$R(\theta,\phi) = \frac{Z_{in}(\theta,\phi) - Z_{in}(0,0)}{Z_{in}(\theta,\phi) + Z_{in}^*(0,0)} \tag{10}$$

And active element gain [15] as,

$$g_r(\theta,\varphi) = \left(4\pi ab/\lambda_0^2\right)\cos(\theta)\left[1 - |R|^2\right] \tag{11}$$

3. RESULTS

The above theory was implemented in a software program for calculating the input impedance, reflection coefficient, efficiency, gain

and pattern of the finite array of circular and rectangular patch antennas. To evaluate the integrals, the cartesian coordinate is first converted into polar coordinate thus converting the double infinite integrals into a finite one [0-2π] and an infinite one [0-∞). Simpson rule integration is used for the finite integral and Gauss quadrature is used for the infinite one. An upper limit of $400k_o$ for the ∞ integral was noticed to provide convergence. Singularity at surface wave modes is also taken into account through residua theory.

In all of the cases considered here, calculations were made with 1 basis functions on both of the circular and rectangular patches for each (ρ, φ) or (x, y) directions and the edge condition was applied to transverse distribution for the aperture and the microstrip feed line. Increase in the number of basis functions, increases the computational time and was shown to have little effects. Numerical convergence tests showed that basis functions corresponding to cavity modes with odd symmetry the so called "Orthogonal set" have very little effects.

Figure 3 shows the magnitude of the reflection coefficient variations versus scanning angle theta in the E-plane, for the central element of two 7×7 arrays, one with circular patches and the other with rectangular patches. In this figure the surface area of the circular and rectangular patches are made equal.

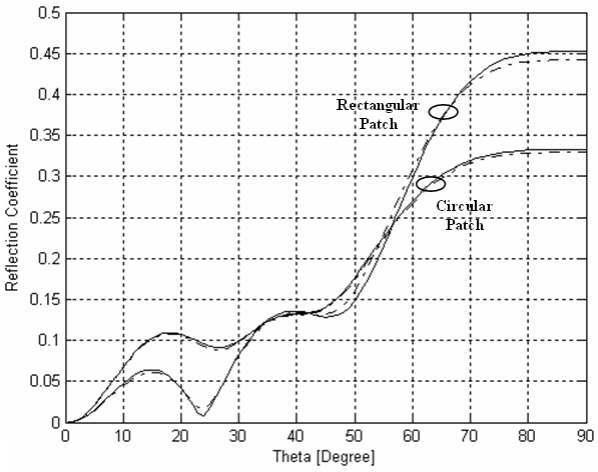

Figure 3. Reflection coefficient magnitude for an array of 7×7 rectangular and 7×7 circular patches with: $\varepsilon_{ra} = 2.55$, $d_a = 0.04\lambda_0$, $\varepsilon_{rf} = 12.8$, $d_f = 0.06\lambda_0$, $L_s = 0.1\lambda_0$, $W_s = 0.01\lambda_0$, $W_f = 0.07\lambda_0$, $L_{Stub} = 0.0$, $a = b = 0.5\lambda_0$, $L_p = 0.3\lambda_0$, $W_p = 0.3\lambda_0$, $r_p = 0.16\lambda_0$. (—) one and ($\cdot-$) two basis functions.

Also shown on this figure, is the effect of increase in the number of basis functions. It is obvious from this result that even with one basis function results converge for both the rectangular and the circular patches. Furthermore, from Fig. 3, the reflection coefficient of the array of circular patches remains less than the array of rectangular patches over the entire scanning angle. This means that array of circular patches has a better performance compared to an array of rectangular patches under the equal patch surface area condition. In the following, the reflection coefficient, efficiency, gain and radiation pattern of the array of aperture coupled circular patches is provided.

The results provided in this paper are pertaining to a series of optimal dimensions and situations which are mainly obtained by tuning the patch sizes and substrate parameters. All the results could be improved by more accurate adjustments.

Figures 4 and 5 shows the reflection coefficient magnitude of the centre element with in an array of circular patches of different size for scanning in the E-plane and H-plane, respectively. Increasing the array size could affect the reflection coefficient by increasing the mutual coupling effects. So the array performance may decrease. As may be seen from these two figures, the blind spot is not a certain problem in the finite arrays; contrarily this is a serious problem in the infinite

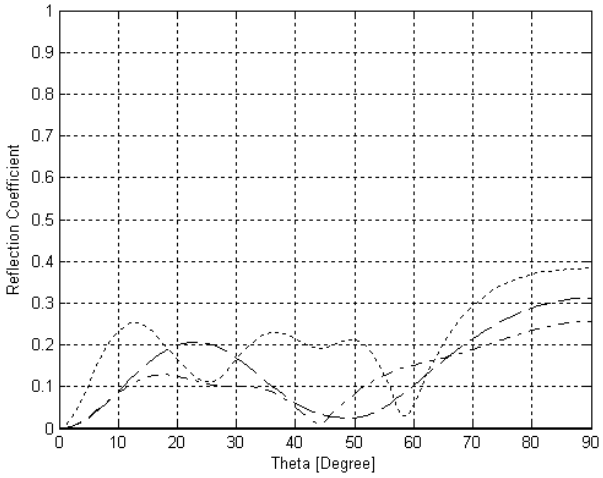

Figure 4. Reflection coefficient magnitude for an array of circular patches with $\varepsilon_{ra} = 2.55$, $d_a = 0.06\lambda_0$, $\varepsilon_{rf} = 12.8$, $d_f = 0.02\lambda_0$, $L_s = 0.115\lambda_0$, $W_s = 0.01\lambda_0$, $W_f = 0.02\lambda_0$, $L_{Stub} = 0.075$, $r_p = 0.13\lambda_0$, $a = b = 0.4\lambda_0$ and with array size of: $(- - -)$ 7×7, $(\cdot -)$ 9×9 and $(\cdots)$ 13×13 in the E-plane.

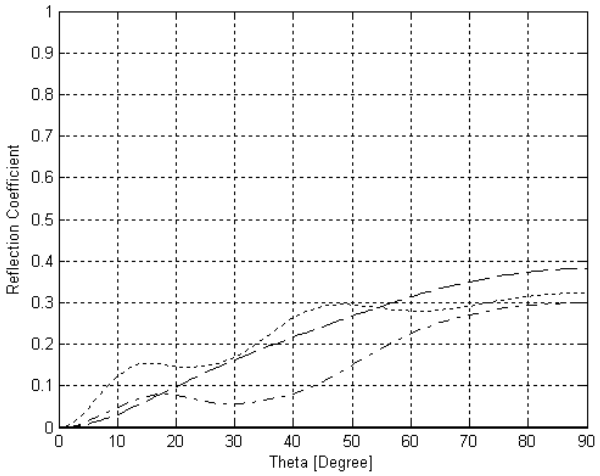

Figure 5. Reflection coefficient magnitude for an array of circular patches with $\varepsilon_{ra} = 2.55$, $d_a = 0.06\lambda_0$, $\varepsilon_{rf} = 12.8$, $d_f = 0.02\lambda_0$, $L_s = 0.115\lambda_0$, $W_s = 0.01\lambda_0$, $W_f = 0.02\lambda_0$, $L_{Stub} = 0.075$, $r_p = 0.13\lambda_0$, $a = b = 0.4\lambda_0$ and with array size of: $(- - -)$ 7×7, $(\cdot -)$ 9×9 and $(\cdots)$ 13×13 in the H-plane.

arrays structure.

In Fig. 6, the efficiency of an array with circular patches is given against scanning angle for the center element of the array as a function of array element separation. It can be seen that by increasing the space between the elements beyond $0.5\lambda_0$, the efficiency decreases dramatically. Similar to Fig. 6, efficiency can be obtained for array scanning in the H-plane. It can be shown that in such a case, efficiency varies between 90–100% for the entire scan range and for various element separations.

For the circular array, Fig. 7 shows the efficiency of the centre element within array of different size. It is clear from this figure that efficiency improves as the array size increases and this is a well known method of increasing the efficiency of single antennas. In the H-plane, the efficiency would remain between 90–100% at the entire scan range; as such it is not drawn here.

The active element gain of the central element of an array with circular patches as a function of array size in the E-plane is shown in Fig. 8. It is clear from this drawing that by increasing the array size, the gain would rapidly boost and this is a common benefit of almost every array.

Figure 9 shows the normalized radiation pattern of the central

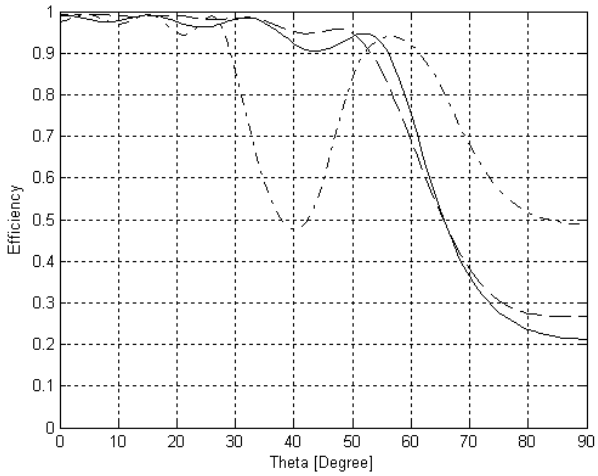

Figure 6. Efficiency for a 9×9 array of circular patches with different patch spacing: $\varepsilon_{ra} = 2.55$, $d_a = 0.06\lambda_0$, $\varepsilon_{rf} = 2.55$, $d_f = 0.05\lambda_0$, $L_s = 0.115\lambda_0$, $W_s = 0.01\lambda_0$, $W_f = 0.17\lambda_0$, $L_{Stub} = 0.075$, $r_p = 0.145\lambda_0$ for: (—) $a = b = 0.4\lambda_0$, $(- - -)$ $a = b = 0.5\lambda_0$ and $(\cdot -)$ $a = b = 0.6\lambda_0$ in the E-plane.

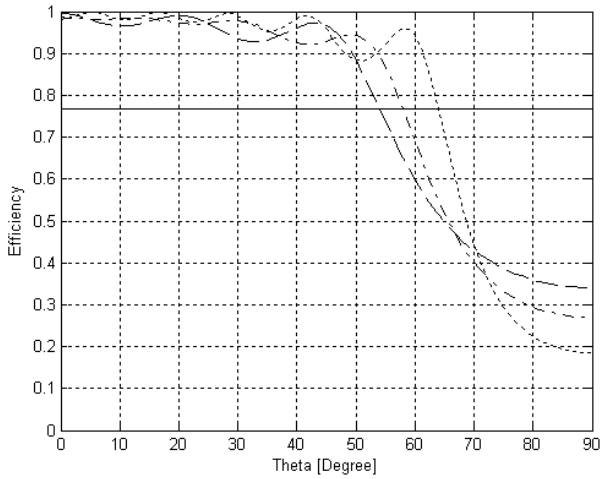

Figure 7. Efficiency for the centre element of an array of circular patches with $\varepsilon_{ra} = 2.55$, $d_a = 0.06\lambda_0$, $\varepsilon_{rf} = 12.8$, $d_f = 0.02\lambda_0$, $L_s = 0.115\lambda_0$, $W_s = 0.01\lambda_0$, $W_f = 0.02\lambda_0$, $L_{Stub} = 0.075$, $r_p = 0.26/2\lambda_0$, $a = b = 0.4\lambda_0$ and with array size of: (—) 1×1, $(- - -)$ 7×7, $(\cdot -)$ 9×9 and $(\cdots)$ 13×13 in the E-plane.

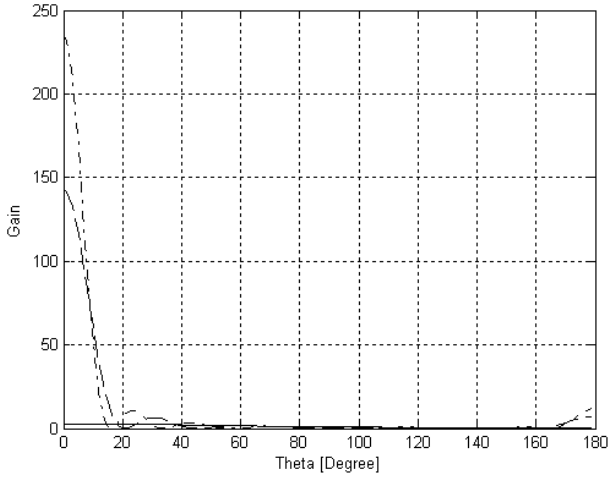

Figure 8. Active element gain for an array of circular patches with $\varepsilon_{ra} = 2.55$, $d_a = 0.06\lambda_0$, $\varepsilon_{rf} = 12.8$, $d_f = 0.02\lambda_0$, $L_s = 0.115\lambda_0$, $W_s = 0.01\lambda_0$, $W_f = 0.02\lambda_0$, $L_{Stub} = 0.075$, $r_p = 0.26/2\lambda_0$, $a = b = 0.4\lambda_0$ and with array size of: (—) 1×1, $(- - -)$ 7×7 and $(\cdot -)$ 9×9 in the E-plane.

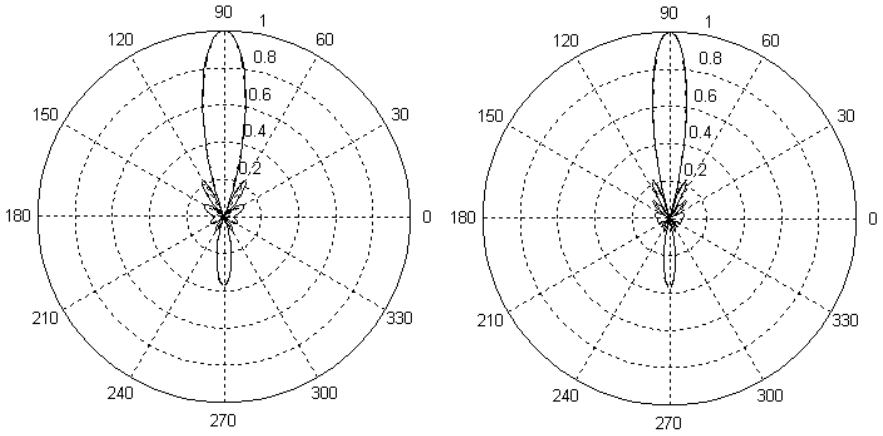

Figure 9. Radiation pattern of a (a) 7×7 and (b) 9×9 array of circular patches with $\varepsilon_{ra} = 2.55$, $d_a = 0.06\lambda_0$, $\varepsilon_{rf} = 12.8$, $d_f = 0.02\lambda_0$, $L_s = 0.115\lambda_0$, $W_s = 0.01\lambda_0$, $W_f = 0.02\lambda_0$, $L_{Stub} = 0.075$, $r_p = 0.13\lambda_0$, $a = b = 0.4\lambda_0$ in the (—) E-plane and $(\cdot -)$ H-plane.

element of a 7×7 and a 9×9 array of circular patches in both the E and H-planes. Once more here, same pattern is achievable for the rectangular patches. Pattern of a 9×9 array is evidently narrower than a 7×7 array which means more directivity and more gain.

4. CONCLUSION

A spectral domain analysis of finite phased array of aperture coupled circular patch antennas has been presented. Results for active input impedance, reflection coefficient magnitude, efficiency, active element gain, and pattern are provided. The effect of array size, element separation and patch dimension on the results has been given both in the E and H-planes. From the results obtained, based on equal patch surface area, it is noted that circular patches provide a better scan performance as compared to the rectangular patches.

ACKNOWLEDGMENT

This work was supported by Engineering & Technology Research Centre of Shahed University.

APPENDIX A.

In the analysis, the required Green's functions are

$$G_{xx}^{EJ} = \frac{jz_0}{4\pi^2 k_0} \cdot \left[\frac{(k_x^2 k_2 \cos k_1 d + jk_x^2 k_1 \sin k_1 d) \cdot \sin k_1 d}{T_e \cdot T_m} - \frac{k_0^2 \sin k_1 d}{T_e} \right]$$

$$G_{xy}^{EJ} = G_{yx}^{EJ} = \frac{jz_0}{4\pi^2 k_0} \cdot \left[\frac{k_x k_y \sin k_1 d}{T_e T_m} (k_2 \cos k_1 d + jk_1 \sin k_1 d) \right]$$

$$G_{yy}^{EJ} = \frac{jz_0}{4\pi^2 k_0} \cdot \left[\frac{(k_y^2 k_2 \cos k_1 d + jk_y^2 k_1 \sin k_1 d) \cdot \sin k_1 d}{T_e \cdot T_m} - \frac{k_0^2 \sin k_1 d}{T_e} \right]$$

$$G_{xy}^{EM} = -G_{yx}^{HJ} = \frac{-jk_x^2(\varepsilon_r - 1) \sin k_1 d}{4\pi^2 T_e T_m} + \frac{k_1}{4\pi^2 T_e}$$

$$G_{yy}^{EM} = -G_{yy}^{HJ} = \frac{-jk_x k_y(\varepsilon_r - 1) \sin k_1 d}{4\pi^2 \cdot T_e T_m}$$

$$\tilde{G}_{yy}^{HM} = \frac{j}{k_0 z_0} \left[\frac{j(\gamma_1 \cos(\gamma_1 d_a) + j\gamma_2 \varepsilon_r \sin(\gamma_1 d_a))(\varepsilon_r k_0^2 - k_y^2)}{\gamma_1 T_m} - \frac{jk_y^2 \gamma_1 (\varepsilon_r - 1)}{T_e T_m} \right]$$

where,

$$\alpha = \arctan\left(\frac{k_y}{k_x}\right) \qquad \beta = \sqrt{k_x^2 + k_y^2}$$

$$T_m = \varepsilon_r k_2 \cos k_1 d + j k_1 \sin k_1 d \qquad T_e = k_1 \cos k_1 d + j k_2 \sin k_1 d$$

The basis functions for the circular patches in the spectral domain are

$$\tilde{\overline{J}}_i(k_x, k_y) = 2\pi r_p j^{-m+1} J_m(\beta_{mn} r_p)$$
$$\left\{ \hat{x} \left[\cos\alpha \cos m\alpha \frac{\beta_{mn}^2}{\beta_{mn}^2 - \beta^2} J'_m(\beta r_p) + m \sin\alpha \sin m\alpha \frac{J_m(\beta r_p)}{\beta r_p} \right] \right.$$
$$\left. + \hat{y} \left[\sin\alpha \cos m\alpha \frac{\beta_{mn}^2}{\beta_{mn}^2 - \beta^2} J'_m(\beta r_p) - m \cos\alpha \sin m\alpha \frac{J_m(\beta r_p)}{\beta r_p} \right] \right\}$$

and for the rectangular patches it is expressed as,

$$\tilde{\overline{J}}_i(k_x, k_y) = \hat{x} \cdot \frac{2k_e(\cos(k_x L/2) - \cos(k_e L/2) - \cos(k_e L/2))}{\sin(k_e L/2) \cdot (k_e^2 - k_x^2)} \cdot \frac{\sin(k_y W/2)}{k_y W/2}$$

where L and W are the patch length and width respectively.

REFERENCES

1. Lee, J. M., W. K. Choi, and C. S. Pyo, "RF integrated aperture coupled array antenna for satellite communication at Ku-band," *IEEE*, 2003.
2. Chamberlain, N., "Microstrip patch antenna panel for large aperture L-band phased array," *IEEE*, 2005.
3. Eldek, A. A., "Design of double dipole antenna with enhanced usable bandwidth for wideband phased array applications," *Progress In Electromagnetics Research*, PIER 59, 1–15, 2006.
4. Eldek, A. A. and A. Z. Elsherbeni, "Rectangular slot antenna with patch stub for ultra wideband applications and phased array systems," *Progress In Electromagnetics Research*, PIER 53, 227–237, 2005.
5. Fu, Y. Q., Q. R. Zheng, Q. Gao, and G. H. Zhang, "Mutual coupling reduction between large antenna arrays using electromagnetic bandgap(EBG) structures," *Journal of Electromagnetic Waves and Applications*, Vol. 20, No. 6, 819–825, 2006.
6. Zhu, Y.-Z., Y.-J. Xie, Z.-Y. Lei, and T. Dang, "A novel method of mutual coupling matching for array antenna design," *Journal of Electromagnetic Waves and Applications*, Vol. 21, No. 8, 1013–1024, 2007.

7. Vescovo, R., "Beam scanning with null and excitation constraints for linear arrays of antennas," *Journal of Electromagnetic Waves and Applications*, Vol. 21, No. 2, 267–277, 2007.
8. Abdelaziz, A. A., "Improving the perforemance of antenna array by using radar absorbing cover," *Progress In Electromagnetics Research Letters*, Vol. 1, 129–138, 2008.
9. Liu, Z. F., P. S. Kooi, L. W. Li, M. S. Leong, and T. S. Yeo, "A method of moments analysis of a microstrip phased array in three layered structures," *Progress In Electromagnetic Research*, PIER 31, 155–179, 2001.
10. Kindt, R. W., K. Sertel, E. Topsakal, and J. L. Volakis, "Array decomposition method for the accurate analysis of finite arrays," *IEEE Transactions on Antennas and Propagation*, Vol. 51, No. 6, June 2003.
11. See, T. S. P. and Z. N. Chen, "Design of stacked offset antenna arrays for ISM-band applications," *Microwave and Optical Technology Letters*, Vol. 39, No. 2, October 2003.
12. Steyskal, H. and J. S. Herd, "Custom modes for microstrip phased array analysis," *Electronics Letters*, Vol. 32, No. 22, October 1996.
13. Yuan, T., L.-W. Li, and M.-S. Leong, "Efficient analysis and design of finite phased arrays of printed dipoles using fast algorithm: some case studies," *Journal of Electromagnetic Waves and Applications*, Vol. 21, No. 6, 737–754, 2007.
14. Pozar, D. M., "Analysis of an infinite phased array of aperture coupled microstrip patches," *IEEE Trans. Antenna Propag.*, Vol. 37, No. 4, 418–425, April 1989.
15. Jang, B.-J., Y.-K. Lee, H.-W. Moon, Y.-J. Yoon, and H.-K. Park, "Analysis of finite phased arrays of aperture-coupled stacked microstrip antennas," *IEEE Transactions on Antennas and Propagation*, Vol. 45, No. 8, August 1997.
16. Aberle, J. T. and D. M. Pozar, "Analysis of infinite arrays of one and two probe fed circular patches," *IEEE Trans. Ant. & Prop.*, Vol. 38, No. 4, 421–432, April 1990.